RSC Advances

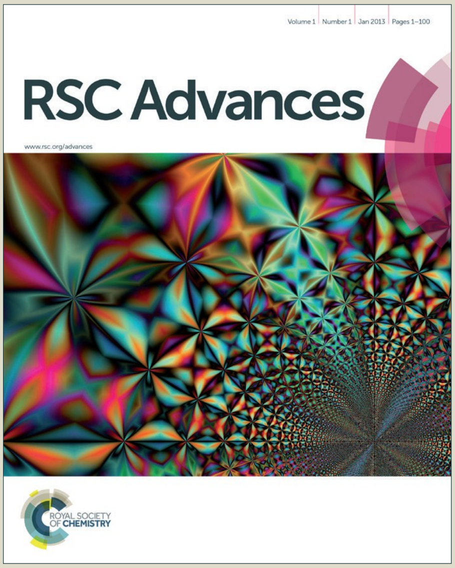

The application of aqueous Ag:ZnInSe quantum-dots on non-toxic sensitized solar cell

Zhao-Chong Wang, Shu-Hong Xu[2]*, Chun-lei Wang, Li Zhu, Fan Bo, Xiao-Yan Lin, Zhu-Yuan Wang, Yi-Ping Cui[1]*

Advanced Photonics Center, School of Electronic Science and Engineering, Southeast University, Nanjing, 210096, China

*Author to whom correspondence should be addressed, E-mail: [1]cyp@seu.edu.cn; [2]xush@seu.edu.cn.

Abstract

We reported the assembly of non-toxic Ag doped ZnInSe (AZIS) quantum dots (QDs) sensitized solar cells with conversion efficiency of 0.89% at 1 sun. The synthesized QDs with the addition of surface active agent (Triton x-100) were directly absorbed on TiO_2 film. ZnS treatment was performed on QDs by Successive Ionic Layer Adsorption and Reaction (SILAR) method to inhibit recombination current of quantum dots sensitized solar cell (QDSSC). The results demonstrated that Triton x-100 increased the loading of QDs on mesoporous TiO_2. By introducing Triton x-100, ZnS passivating layer and Cu_2S counter electrode, the conversion efficiency of aqueous and non-toxic AZIS QDSSC reached 0.89% at 1 sun.

Keywords: AZIS QDSSC; Triton x-100; aqueous; non-toxic.

1. Introduction

QDSSCs have attracted much attention in recent decades for their photo-stability of inorganic material, high molar extinction coefficients and facile tunability of band gaps. The use of QDs as sensitizers was proposed by Zaban *et al.* in 1998.[1] In QDSSC, excited sensitizer generated electrons and holes, which were split and injected into the semiconductor (e.g.TiO_2) and the hole-transporter respectively. Photoelectrons were transferred through the conductive glass and the external circuit, and recombined with holes at cathode, forming a complete circuit. Recently, Cd-containing QDs sensitized solar cell, reported by Wang *et al*,[2] achieved the conversion efficiency of 6.76% at 1 sun.

However, the reported sensitizer of QDSSC mostly contained the cadmium chalcogenide compounds such as CdS and CdSe,[3] as well as the lead chalcogenide compounds such as PbS and PbSe.[4] There existed two main problems for these kinds of QDSSC. First, the intrinsic toxicity of Cd or Pb contained QDs has arisen as a major issue for the prospects of commercialization. Second, most QDSSC were sensitized by the QDs synthesized via organometalic methods.[5] These methods required high synthesis temperature and entailed ligand exchange process. QDs synthesized in water, which were simpler in preparation process and closer to the principle of green chemistry, were relatively scarcely applied as sensitizer. The major obstacles of application of aqueous QDs as solar cell were low loading amount of QD and low conversion efficiency.

As for aqueous QDs sensitized solar cell, there were two methods to anchor QDs on TiO_2. First one was in situ loading approach, including growth of QDs by chemical bath deposition (CBD),[6, 7] successive ionic layer adsorption and reaction (SILAR),[8, 9] which could obtain a high loading of QDs. However, it was difficult to control the size, chemical composition and surface properties of QDs with these methods. Second one was ex situ loading approach, namely deposition of pre-synthesized colloidal QDs by linker-assisted adsorption (LA).[10, 11] In this method band gaps of QDs could be accurately controlled. A full and even coverage of sensitizer onto a mesoporous TiO_2 was crucial for the development of QDSSC performance. However loading of QDs on mesoporous TiO_2 was generally poor. Many methods have been developed to enhance the loading of QDs. Our group has reported that loading of linker capped CdTe QDs on mesoporous TiO_2 could be effectively improved via pH-control and switching strong alkaline loading environment.[12, 13]

In this paper, non-toxic and aqueous AZIS QDs were absorbed onto TiO_2 with linker-assisted adsorption. Via utilizing surface active agent (Triton x-100), ZnS passivating layer and Cu_2S counter electrode, the conversion efficiency of AZIS QDSSC reached 0.89% at 1 sun. Besides, fabrication process of AZIS QDSSC was optimized and effect of ZnS layer was analyzed via impedance spectrum.

2. Experimental section

2.1 Synthesis of Ag:ZnInSe QDs

Ag:ZnInSe QDs colloidal dispersion was prepared according to our previous work.[14] Namely, the mixture of $Zn(NO_3)_2$, $AgNO_3$, $In(NO_3)_3$ and MPA was adjusted to pH 8.0 by using NaOH solution. Freshly prepared NaHSe solution was injected into the mixture after the solution was aerated with N_2 for 30min. The total concentration of Zn and In in the mixture was 0.01M. Molar ratio of Zn:In:Ag:Se:MPA was about 3:1:0.12:0.8:8. Then, the solution was refluxed at 100°C for 6h. The as prepared QDs colloidal dispersion was condensed to 20 times of original concentration with rotary evaporator.

2.2 Preparation of the TiO_2 photoanode

Prior to the fabrication of TiO_2 photoanode, fluorine-doped tin oxide (FTO) glass was ultrasonically cleaned sequentially for 10min in detergent, water, 2-propanol, and acetone. Mesoporous TiO_2 films were prepared by screen printing of aqueous slurry of Degussa P25 nanoparticles on the FTO glass. A paste for the scattering layer containing anatase TiO_2 particles was deposited by screen printing, forming light scattering TiO_2 films. This was followed by sintering at 450 °C for 30 min. The thickness of the TiO_2 films was 20μm, including active layer (14μm) and scattering layer (6μm). The area of the TiO_2 films was approximately $0.36cm^2$ (0.6cm×0.6cm square).

2.3 AZIS coated on TiO_2 films and glass

Sensitization of TiO_2 samples by direct adsorption of AZIS QDs was carried out by immersing the oxide films in 3.5ml condensed QDs suspension. Different weight of Triton X-100 was added to improve the loading of QDs. The TiO_2 film turned brown after immersion for 48h, indicating the loading of AZIS QDs on TiO_2.

2.4 Surface post-treatment: ZnS treatment

To further reduce the recombination of photoelectrons, a thin ZnS layer was coated onto the QD-loaded TiO_2 electrode by the SILAR method. This procedure, repeated 3 times, entailed consecutively dipping sensitized samples in a 0.1M $Zn(NO_3)_2$ ethanol solution and a 0.1M Na_2S ethanol solution for 1 min, washing thoroughly with water between immersions to remove the excess of non-adsorbed/unreacted ions.

2.5 Assembly of the QDSSC

After coated with AZIS QDs, the TiO_2 electrode was assembled by sandwiching with Pt counter electrode and sealed with a silicone spacer (thickness ~60um). The polysulfide electrolyte, consisting of 0.5M Na_2S, 2M S and 0.2M KCl in methanol/water (7:3 by volume), was used in this work.

2.6 Characterization

All optical measurements were performed at room temperature under ambient conditions. UV–Vis absorption spectra (UV) were recorded with a Shimadzu 3600 UV–Vis near-infrared spectrophotometer. The morphology and chemical composition of photoanode were examined by HitachS-4800 field-emission scanning electron Microscopy (SEM) equipped with an energy dispersive X-ray spectrometer (EDS) analyzer (Bruker). For *J*-V curve measurement, a solar simulator (model 66902) from Newport, which has a 450W xenon lamp with an irradiance of $100mW/cm^2$ (equivalent to one sun at AM 1.5) at the surface of the solar cell, was used. The incident photon to current conversion efficiency (IPCE) was measured with a 300W xenon lamp and a lock-in amplifier (Oriel) in the wavelength range of 300–800nm. Electrochemical impedance spectra (EIS) measurements were carried out by applying a 10mV AC signal over the frequency range of 0.1Hz to 100kHz under dark condition at various bias voltages by using a CS350 electrochemical workstation (CorrTest).

3. Results and discussion

Water soluble, as-prepared Ag:ZnInSe quantum dots were directly absorbed onto the mesoporous TiO_2. Ag:ZnInSe QDs colloidal dispersion was prepared by reflux at 100°C for 6h. TiO_2 films were prepared by screen printing of TiO_2 particles on FTO and sintering at 450°C. QDs were loaded on TiO_2 via immersing TiO_2 film in AZIS suspension. Unfavorable QDs loading was achieved under the effect of electrostatic repulsion and Van der Waals forces between TiO_2 and QDs.[12] Surface active agent was added in QDs suspension to enhance the absorption (scheme 1). ZnS passivation layer was coated onto TiO_2 and QDs to reduce recombination of QDSSCs.

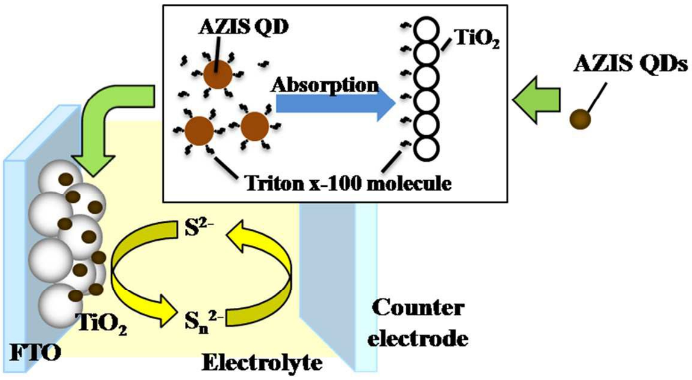

Scheme 1. Structure and fabrication process of AZIS QDSSCs. Non-toxic AZIS QDs were directly absorbed onto TiO_2 film. Triton x-100 was used to enhance absorption of AZIS QDs.

Figure 1 showed the optical absorption spectrum of QDs sensitized photoanodes added with different weight of Triton x-100. All photoanodes were immersed in QDs suspension for 48 hours. For TiO_2 and TiO_2/QDs sample (black and green line in Figure 1), the absorbance of TiO_2 was obviously improved after being immersed in QD suspension, indicating the effective loading of QDs onto TiO_2. Figure 2 showed absorption spectrum of sample added 30mg Triton x-100. The absorption spectrum of TiO_2 was deducted. The results accorded with the absorption spectrum of AZIS QDs reported by Wang *et al*[14], which covered 400-700nm. IPCE spectrum was depicted in the insert of Figure 2. Obvious quantum efficiency (QE) of AZIS QDSSC could be observed during 400-600nm, which proved that AZIS QDs could absorb photons and transferred photons into electrons in 400-600nm.

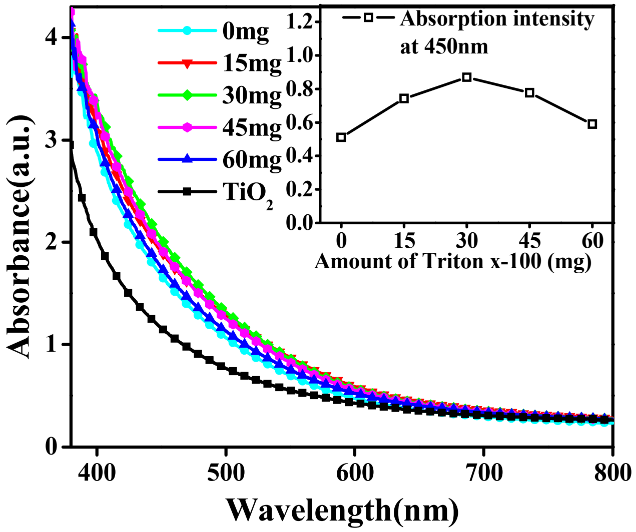

Figure 1. Absorption spectra of TiO_2 and TiO_2/QDs samples fabricated with different weight of Triton x-100 (0mg, 15mg, 30mg, 45mg, and 60mg). The corresponding Triton x-100 concentrations of these samples were 0mM, 0.16mM, 0.32mM, 0.48mM, and 0.64mM. The inset showed absorption intensity at 450nm of TiO_2/QDs samples.

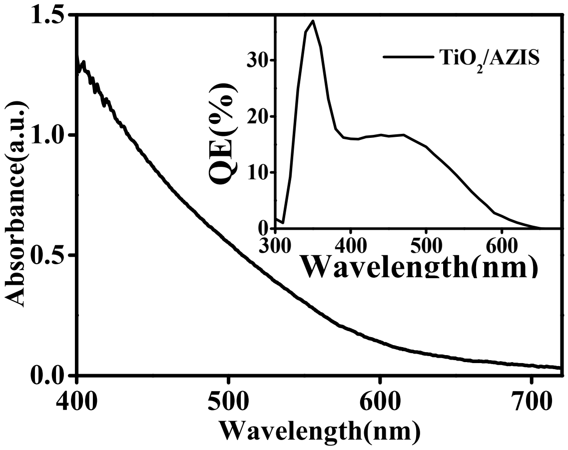

Figure 2. Absorption spectrum of TiO$_2$/QDs sample fabricated with 30mg Triton x-100. Absorption intensity of TiO$_2$ has been deducted. Corresponding IPCE spectrum of TiO$_2$/QDs sample was shown in the inset. Pt counter electrode and polysulfide electrolyte were used to form a sandwich-type configuration.

Absorption intensity at 450nm of samples with different weight Triton x-100 was shown in the inset of Figure 1. The absorption intensity of TiO$_2$ was deducted. Absorption intensity of sensitized photoanodes increased with the amount of Triton x-100 increasing from 0mg to 30mg. Then the intensity decreased in the range 30-60mg. The sample with 30mg Triton x-100 had the best absorbance. The trend of absorption intensity at 450nm indicated that the weight of Triton x-100 added in suspension had impact on loading quantity of QDs on photoanode. Maximum loading of QDs was achieved when 30mg Triton x-100 was added, resulting in highest absorption intensity.

Liquid electrolyte based solar cells were assembled by sandwiching a prepared

AZIS QDs sensitized TiO_2 film and a Pt counter electrode, using a silicone spacer (thickness ~60 um), and a droplet (20uL) of polysulfide electrolyte. The results of photocurrent–voltage (*J*–V) curves of AZIS QDs sensitized solar cells with various amount of Triton x-100 has been depicted in Figure 3. Each TiO_2 film was immersed in the condensed QDs colloidal dispersion for 48 hours. Table 1 listed the photovoltaic parameters. Obviously, the short-circuit current density (*J*sc) and the open-circuit voltage (V_{OC}) increased as the amount of Triton x-100 increased, reaching maximum value of 2.7mA/cm^2 and 0.48V at 30mg. When more Triton x-100 (more than 30mg) was added, *J*sc and Voc started to decrease. On the other hand, the fill factor (FF) increased from 0.37 to 0.40 when addition of Triton x-100 increased from 0mg to 15mg. Then it remained relatively constant (0.39-0.40) in the range of 15-45mg. Finally it decreased to 0.35 when 60mg Triton x-100 was added. With increasing amount Triton x-100, the conversion efficiency (η) firstly increased and then decreased after reaching a maximum value of 0.50% at 30mg. Consequently, the photovoltaic parameters of QDSSC were optimal when 30mg Triton x-100 was added. The conversion efficiency of QDSSC with 30mg addition was improved by 32% compared with that of QDSSC fabricated without Triton x-100.

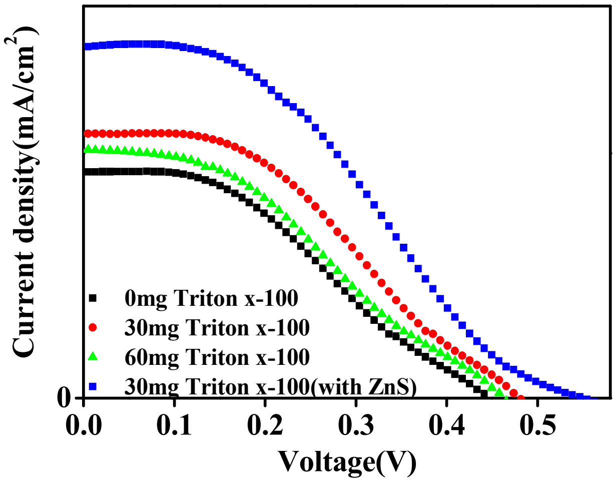

Figure 3. *J* –V curves of AZIS QDSSCs fabricated with 0mg, 30mg (with and without ZnS passivating layer) and 60mg addition of Triton x-100. The concentrations of Triton x-100 corresponding to 0mg, 30mg, and 60mg addition were 0mM, 0.32mM， and 0.64mM respectively.

Table1. Photovoltaic parameters of AZIS QDSSCs fabricated with 0mg, 15mg, 30mg (with and without ZnS passivating layer), 45mg, and 60mg addition of Triton x-100. The concentrations of Triton x-100 corresponding to 0mg, 15mg, 30mg, 45mg, and 60mg addition were 0mM, 0.16mM, 0.32mM, 0.48mM, and 0.64mM respectively.

Weight of Triton x-100(mg)	Voc(V)	*J*sc(mA/cm^2)	FF	η(%)
0	0.44	2.31	0.37	0.38
15	0.46	2.48	0.40	0.46
30	0.48	2.70	0.39	0.50
45	0.47	2.46	0.40	0.46
60	0.46	2.52	0.35	0.41
30(with ZnS)	0.55	3.56	0.36	0.71

From the above analysis, it has been found that QDSSC with 30mg Triton x-100 showed the maximum QDs loading as well as the highest photocurrent. The highest QDs loading quantity resulted in most compact QDs layer on TiO_2 surface, which increased Voc as well as FF.[15] Energy dispersive spectrometer (EDS) was employed to test the loading quantity of QDs. Atoms ratios of Se-to-Ti at different depths of samples with 0mg, 30mg, and 60mg Triton x-100 were measured from EDS (Figure 4). The thickness of the TiO_2 films was 20μm determined from the SEM images inserted in Figure 4. The value of Se-to-Ti ratio of the three samples remained relatively stable in the range of 2-20μm, indicating the uniform distribution of QDs in mesoporous TiO_2. SEM images of TiO_2 photoanode from the cross-sectional view along with enlarged image of scattering layer was presented in Figure S1. QD loading ability on mesoporous TiO_2 was closely related to the size of TiO_2 particles. The scattering layer was observed to be a mixture of large TiO_2 spherical particles and smaller TiO_2 nanoparticles. Therefore, QDs loadings on scattering layer (range of 2-6μm) of the three samples were not much different from that on active layer. Similar phenomenon of the mixed scattering layer was reported by Zhou *et al.*[16]

Furthermore, Se-to-Ti atom ratio of sample fabricated with 30mg Triton x-100 was higher than those of other two samples. The average atom ratio at each depth were calculated and illustrated in the insert map. Apparently average Se-to-Ti atom ratio increased when amount of Triton x-100 increased from 0mg to 30mg, showing higher loading of QDs in TiO_2. However, loading of QDs decreased to lower level of sample with 60mg Triton x-100. This trend confirmed that the 30mg Triton x-100 improved the loading of QDs, while excessive concentration (more than 0.32mM) of Triton x-100 reduced the loading quantity.

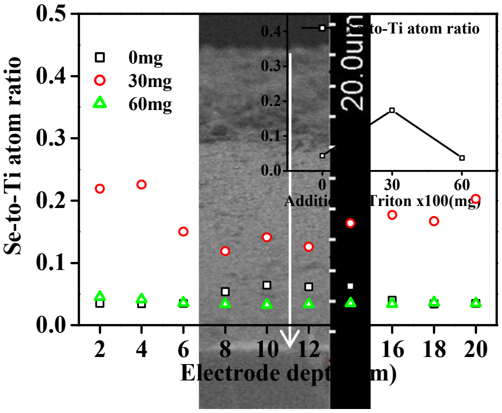

Figure 4. Atoms ratio of Se-to-Ti at different depths (from 2μm to 20μm) of QDs sensitized photoanodes with 0mg, 30mg, and 60mg Triton x-100. Insert map shows SEM image and average ratios with 0mg, 30mg, and 60mg addition of Triton x-100. The concentrations of Triton x-100 corresponding to 0mg, 30mg, and 60mg addition were 0mM, 0.32mM, and 0.64mM respectively.

Scheme 2 indicated the loading process of QDs with Triton x-100. When the amount reached 30mg, the concentration of Triton x-100 in the solution was 0.32Mm, which was close to the critical micelle concentration (cmc) of Triton x-100 (0.27mM).[17] As shown in Scheme 2(a), Triton x-100 existed in the configuration of single molecule when its concentration was below cmc. Triton x-100 capped QDs tended to absorb on the surface of TiO_2 according to the hydrophobic interaction, leading to the increase of QDs loading on mesoporous TiO_2. In comparison, configuration of Triton x-100 tended into micelle when its concentration was above cmc (Scheme 2(b)). The micelle capped QDs tended to disperse in the solution rather than absorbing on the mesoporous TiO_2. Consequently, the highest loading of QDs was achieved in the concentration close to cmc (namely 30mg addition). The higher loading of QDs can hinder nanochannels of some parts of mesoporous TiO_2, which may explain that QDs distribution in sample of 30mg was less uniform than other two samples.

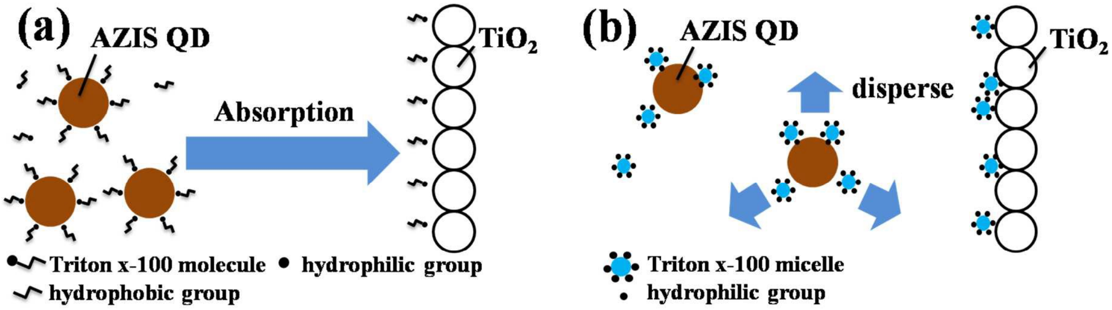

Scheme 2. The process of AZIS QDs loading on mesoporous TiO_2 in solution with the concentration of Triton x-100 (a) below and (b) above cmc.

The absorption intensity in 450nm of AZIS QDs sensitized photoanodes based on different absorption times was showed in Figure 5. All samples were fabricated with 30mg Triton x-100. The absorption intensity of sensitized photoanode increased sharply during 0-24 hours. Then it went up slightly during 24-48 hour. When absorption time was more than 48h, the absorption intensity maintained almost unchanged, indicating a balanced state of absorption process. Therefore 48 hours was considered sufficient for QDs absorbed onto mesoporous TiO_2.

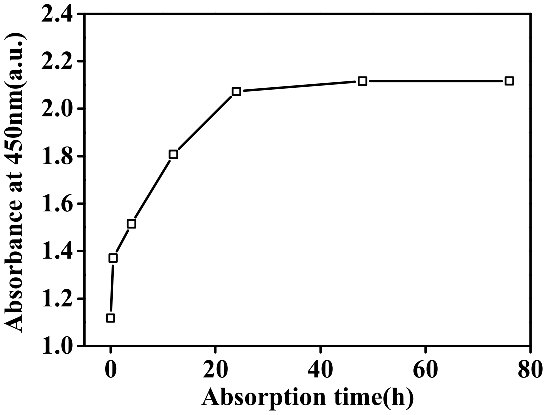

Figure 5. Absorption intensity at 450nm of QDs sensitized photoanodes with absorption time ranging from 0h to 72h. 30mg Triton x-100 was add in the absorption solution.

In addition, we have measured photovoltaic performance of QDSSC sensitized by ZnInSe (ZIS) QDs. *J*-V curves of ZIS and AZIS QDSSCs were illustrated in Figure S2. V_{OC}, J_{SC} and conversion efficiency of ZIS QDSSC were far behind those of AZIS QDSSC. Ag doping in the ZIS QDs introduced anion vacancies and provided an intermediate level between the conduction band of ZnInSe and TiO_2.[18] A gradient alignment of energy level, which was favorable for the transport of photoelectrons, was formed in the sensitized photoanode.[19]

The effect of ZnS surface treatment on AZIS QDSSC has been investigated. Sensitized photoanode with 30mg Triton x-100 was submitted to 3 SILAR of ZnS treatments (assembled with Pt electrode), forming a sandwich-type configuration. Polysulfide electrolyte was used as the hole transporting medium. *J*-V curve of the ZnS coated QDSSC was presented in Figure 3 (blue line). Parameters of this QDSSC were listed in Table 1. J_{sc} and V_{OC} of the sample with 30mg Triton x-100 were evidently increased after ZnS coating. Specifically, V_{OC} increased from 0.48V to 0.55V, and J_{SC} increased from 2.70mA to 3.56mA. Conversion efficiency was dramatically increased by 42%, reaching 0.71% after the ZnS coating. The ZnS layer could effectively passivate the surface states of QDs and TiO_2. Electron leakage at TiO_2/electrolyte interface was inhibited, which was believed responsible for enhancement of V_{OC} and J_{SC}.[20] On the other hand, FF of the coated sample decreased from 0.39 to 0.36, which was caused by the blocking of the mesoporous TiO_2 and the inhibition of the electrolyte saturation by ZnS coating, as reported by Shen *et al*. [21]

Recombination resistance (Rr) at TiO_2/electrolyte interface of AZIS QDSSCs was measured by EIS. Solar cells were assembled into a sandwich-type configuration and applied with various biases. Rr of samples under different bias was extracted by fitting Nyquist plots with the equivalent circuit described by Gonzàlez-Pedro *et al*.[22] Figure 6 presented the Nyquist plots of samples with and without ZnS layer under bias of -0.4V. Experimental data and resulting fitting curves were illustrated in spots and solid lines respectively. It was observed that fitting curves matched well with testing results. The larger arc in Nyquist plot, which represented the scale of Rr, increased after ZnS coating. Rr of the samples as a function of the bias was presented in Figure 7. Decrease in recombination resistance with the increase of bias was caused by upward shift of the TiO_2 Fermi level under higher bias.[20] Rr of sample increased after ZnS coating under each bias, which indicated lower recombination current at TiO_2/electrolyte interface.

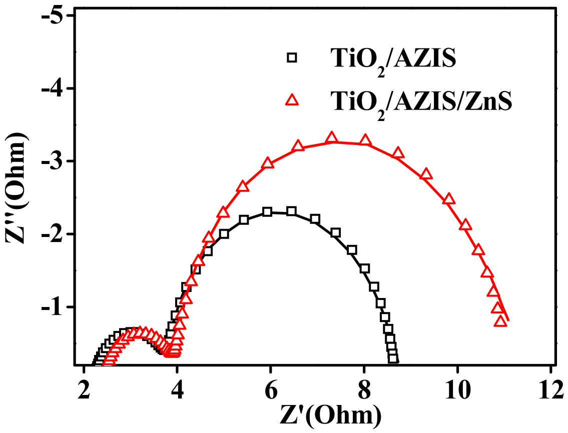

Figure 6. Nyquist plots of AZIS QDSSCs with and without ZnS passivating layer. Samples were fabricated with 30mg Triton x-100 and 48 hours absorption time.

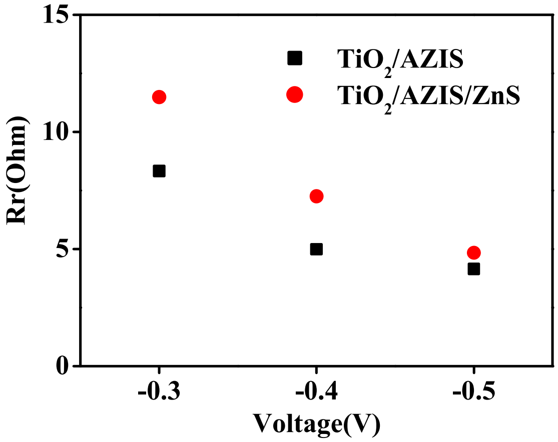

Figure 7. Recombination resistance of samples as a function of their bias. Samples were fabricated with 30mg Triton x-100 and 48 hours absorption time.

From the table 1, the FFs of the AZIS QDSSCs with Pt counter electrode ranged from 0.35 to 0.40. The unfavorable FFs were attributable to resistance losses in the device, including losses in each interface and in the electrolyte. As we have known that Pt counter electrode was not an ideal catalyst for the polysulfide redox reaction, which contributed to the poor FF of the cell. In order to achieve a higher FF and conversion efficiency, Pt electrode was substituted with Cu_2S counter electrode. Figure 8 showed the *J*-V curve and photovoltaic parameters of the sample using Cu_2S electrode and fabricated under optimal condition. FF was increased from 0.36 to 0.57. Higher conversion efficiency of 0.89% at 1 sun was obtained.

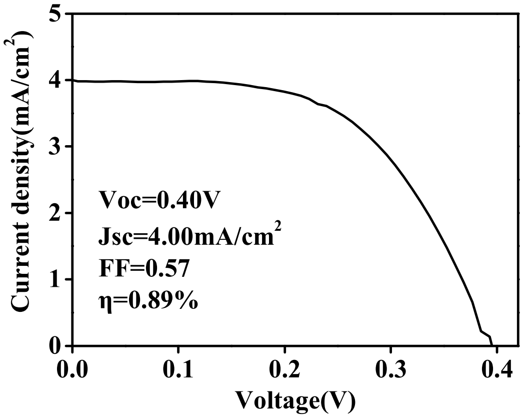

Figure 8. *J*-V curve of AZIS QDSSC fabricated with 30mg addition of Triton x-100, 48-hour absorption time and 3 SILAR of ZnS coating. Cu_2S was used as counter electrode.

Compact coverage QDs of onto mesoporous TiO_2 network, suppression of electron recombination and catalytic capability of counter electrode were crucial factors for development of QDSSCs performance. The absorption spectrum and EDS showed that maximum AZIS QDs were loaded onto TiO_2 photoanode when 30mg Triton x-100 was added in suspension. EIS confirmed that recombination at the TiO_2/electrolyte interface was reduced by ZnS treatment. With optimal process (namely 30mg addition of Triton x-100, 48-hour absorption time, 3 SILAR of ZnS coating and usage of Cu_2S electrode), the highest efficiency we achieved of AZIS QDSSC was 0.89% at 1 sun. Besides, we avoided the ligand exchange process by synthesizing and loading MPA capped AZIS QDs in aqueous solution, which made AZIS QDSSC an alternative of nontoxic, easy-fabricated and efficient QDSSCs.

4. Conclusion

Non-toxic Ag:ZnInSe QDSSC was successfully assembled by process of linker-assisted direct adsorption. Triton x-100 was used to improve the loading of QDs onto mesoporous TiO_2. Favorable loading of QDs was achieved with 30mg Triton x-100 in solution. Recombination current of QDSSC was inhibited by ZnS passivating layer. Finally, with immersion of TiO_2 film in QDs suspension for 48 hours, addition of 30mg Triton x-100, coating of ZnS and using of Cu_2S electrode, the efficiency of QDSSC reached 0.89% at 1 sun. A non-toxic QDSSC as well as a convenient way of improving QDs loading was introduced in this report.

Acknowledgements

This work is supported by the National Key Basic Research Program of China (Grant No. 2015CB352002), National Natural Science Foundation of China (Grant Nos. 61475034, 21403034, 61177033), the Fundamental Research Funds for the Central Universities (No. 2242014R30006), and the natural science foundation of Jiangsu Province Youth Fund (No. BK20140650), China Postdoctoral Science Foundation (No. 2014M560370), Jiangsu Planned Projects for Postdoctoral Research Funds (No. 1401035B).

References

1. A. Zaban, O. I. Micic, B. A. Gregg and A. J. Nozik, *Langmuir*, 1998, 14, 3153-3156.
2. J. Wang, I. Mora-Sero, Z. X. Pan, K. Zhao, H. Zhang, Y. Y. Feng, G. Yang, X. H. Zhong and J. Bisquert, *J. Am. Chem. Soc.*, 2013, 135, 15913-15922.
3. J. Debgupta, S. Mandal, H. Kalita, M. Aslam, A. Patra and V. Pillai, *RSC Adv.*, 2014, 4, 13788-13795.
4. D. Ding, Y. L. Chen, P. Lv, H. Z. Yao, Y. N. Mu, S. Su, X. L. Zhang, L. Y. Zhou, W. Y. Fu and H. B. Yang, *RSC Adv.*, 2015, 5, 6462-6469.
5. J. H. Park, S. J. Kang, S. Kim, H. Lee and J. S. Lee, *RSC Adv.*, 2014, 4, 51471-51476.
6. Y. L. Lee and Y. S. Lo, *Adv. Funct. Mater.*, 2009, 19, 604-609.
7. C. S. Kim, S. H. Choi and J. H. Bang, *ACS Appl. Mater. Interfaces*, 2014, 6, 22078-22087.
8. H. Lee, M. K. Wang, P. Chen, D. R. Gamelin, S. M. Zakeeruddin, M. Gratzel and M. K. Nazeeruddin, *Nano Lett.*, 2009, 9, 4221-4227.
9. C. Chen, Q. L. Dai, C. Miao, L. Xu and H. W. Song, *RSC Adv.*, 2015, 5, 4844-4852.
10. N. Guijarro, T. Lana-Villarreal, I. Mora-Sero, J. Bisquert and R. Gomez, *J. Phys. Chem. C*, 2009, 113, 4208-4214.
11. W. J. Li, Z. X. Pan and X. H. Zhong, *J. Mater. Chem. A*, 2015, 3, 1649-1655.
12. X. Y. Lin, C. L. Wang, S. H. Xu and Y. P. Cui, *J. Phys. D-Appl. Phys.*, 2014, 47.
13. F. Bo, C. L. Wang, S. H. Xu, C. F. Zhang, Z. Y. Wang and Y. P. Cui, *J. Phys. D-Appl. Phys.*, 2014, 47.
14. C. L. Wang, S. H. Xu, Y. J. Shao, Z. Y. Wang, Q. Y. Xu and Y. P. Cui, *J. Mater. Chem. C*, 2014, 2, 5111-5115.
15. K. Y. Yan, W. Chen and S. H. Yang, *J. Phys. Chem. C*, 2013, 117, 92-99.
16. R. Zhou, Q. F. Zhang, E. Uchaker, L. Yang, N. Q. Yin, Y. H. Chen, M. Yin and G. Z. Cao, *Electrochim. Acta*, 2014, 135, 284-292.
17. C. U. Herrmann and M. Kahlweit, *J. Phys. Chem.*, 1980, 84, 1536-1540.
18. E. Hao, Y. P. Sun, B. Yang, X. Zhang, J. M. Liu and J. C. Shen, *J. Colloid Interface Sci.*, 1998, 204, 369-373.
19. L. Yang, R. Zhou, J. L. Lan, Q. F. Zhang, G. Z. Cao and J. G. Zhu, *J. Mater. Chem. A*, 2014, 2, 3669-3676.
20. I. Mora-Sero, S. Gimenez, F. Fabregat-Santiago, R. Gomez, Q. Shen, T. Toyoda and J. Bisquert, *Accounts Chem. Res.*, 2009, 42, 1848-1857.
21. Q. Shen, J. Kobayashi, L. J. Diguna and T. Toyoda, *J. Appl. Phys.*, 2008, 103.
22. V. Gonzalez-Pedro, X. Q. Xu, I. Mora-Sero and J. Bisquert, *ACS Nano*, 2010, 4, 5783-5790.